

IEEE

ANTENNAS AND WIRELESS PROPAGATION LETTERS

A PUBLICATION OF THE IEEE ANTENNAS AND PROPAGATION SOCIETY



DECEMBER 2018

VOLUME 17

NUMBER 12

IAWPA7

(ISSN 1536-1225)

LETTERS

A Reader Antenna for UHF Near-Field RFID Applications Based on the Segment-Line Oppositely Directed Currents C. Huang, C. Wang, J. Zhu, and W. Tang	2159
Classification of Indoor Environments for IoT Applications: A Machine Learning Approach M. I. AlHajri, N. T. Ali, and R. M. Shubair	2164
Analysis of Graphene-Based Devices Using Wave Equation Based Discontinuous Galerkin Time-Domain Method P. Wang, Y. Shi, C.-Y. Tian, and L. Li	2169
A Weak-Form Combined Source Integral Equation With Explicit Inversion of the Combined-Source Condition J. Kornprobst and T. F. Eibert	2174
A Broadband Circularly Polarized High-Temperature Superconductor Microstrip Antenna for Space Applications X. Zeng, Z. Hu, Q. Chen, X. Wei, and K. Huang	2179
Measurement of the Antenna Phase Center Position in Anechoic Chamber C. Esposito, A. Gifuni, and S. Perna	2183
A Self-Packaged Circularly Polarized Dielectric Resonator Antenna With Wide Bandwidth and High Gain W.-W. Yang, X.-Y. Dong, Y.-L. Li, and J.-X. Chen	2188
Wideband RCS Reduction of a Slot Array Antenna Using Phase Gradient Metasurface W. Zhang, Y. Liu, S. Gong, J. Wang, and Y. Jiang	2193
Wideband Radiation From an Offset-Fed Split Ring Resonator With Multi-Order Resonances L. Peng, S. Sang, Z. Wang, H. Jin, A. Wu, K. Xu, and G. Wang	2198
Multiple-Frequency CW Radar and the Array Structure for Uncoupled Angle-Range Indication B. Chen, Y. Huang, X. Chen, G. Wang, and J. Guan	2203
Analysis of Reflectarray Antenna Elements Under Arbitrary Incident Angles and Polarizations Using Generalized Boundary Conditions X. Liu, F. Yang, M. Li, and S. Xu	2208
Multilayer Dielectric End-Fire Antenna With Enhanced Gain D. C. Lugo, R. A. Ramirez, J. Wang, and T. M. Weller	2213
E-Textile Origami Dipole Antennas With Graded Embroidery for Adaptive RF Performance S. Alharbi, S. Chaudhari, A. Inshaar, H. Shah, C. Zou, R. L. Harne, and A. Kiourti	2218
A NRI-TL Metamaterial Leaky-Wave Antenna Radiating at Broadside With Zero Beam-Squinting K. M. Kossifos and M. A. Antoniadis	2223
A Spherical Aberration Corrective Lens for Centimeter Through Submillimeter Wavelength Antennas P. F. Goldsmith and M. Alonso-DelPino	2228
Broadband Quasi-Bidirectional Antenna With Vertical Polarization R. Wang, B.-Z. Wang, and X. Ding	2232
Design of Wideband Bowtie Slot Antenna Using Sectorially Modified Gielis Curves V. S. Bhaskar, E. L. Tan, and L. K. H. Holden	2237
Computation of Two-Dimensional Green's Function for Arbitrary Shaped Multilayer Cylinders T. U. Gürbüç	2241

(Contents Continued on Page 2157)



Enhanced Transmission Through Single Subwavelength Apertures Using Miniaturized Planar Resonators	S. N. Azemi and W. S. T. Rowe	2246
Indoor Small-Scale Spatiotemporal Propagation Characteristics at Multiple Millimeter-Wave Bands	P. Zhang, J. Li, H. Wang, H. Wang, and W. Hong	2250
Microfluidically Polarization-Switchable Metasurfaced Antenna	A. H. Naqvi and S. Lim	2255
Measurement of Attenuation by Building Structures in Cellular Network Bands	S. S. Zhekov, Z. Nazneen, O. Franek, and G. F. Pedersen	2260
Wideband Low Axial Ratio and High-Gain Sequentially Rotated Antenna Array	W. Hu, D. Inserra, G. Wen, and Z. Chen	2264
Design of Multiple-Polarization Reflectarray for Orbital Angular Momentum Wave in Radio Frequency	X.-S. Meng, J.-J. Wu, Z.-S. Wu, T. Qu, and L. Yang	2269
Calculation Method for Evaporation Duct Profiles Based on Artificial Neural Network	X. Yan, K. Yang, and Y. Ma	2274
Millimeter-Wave Beam-Tilting Vivaldi Antenna With Gain Enhancement Using Multilayer FSS	M. B. Kakhki, M. Mantash, A. Kesavan, M. M. Tahseen, and T. A. Denidni	2279
Mutual Coupling Reduction for a UWB Coplanar Vivaldi Array by a Truncated and Corrugated Slot	Nurhayati, G. Hendranto, T. Fukusako, and E. Setijadi	2284
Wideband Planarized Dual-Linearly-Polarized Dipole Antenna and Its Integration for Dual-Circularly-Polarized Radiation	H.-H. Sun, H. Zhu, C. Ding, and Y. J. Guo	2289
An Accelerated SBR for EM Scattering From the Electrically Large Complex Objects	C.-L. Dong, L.-X. Guo, X. Meng, and Y. Wang	2294
Two-Dimensional Dynamic Metasurface Apertures for Computational Microwave Imaging	M. F. Imani, T. Sleasman, and D. R. Smith	2299
Wide Solid Angle Beam-Switching Conical Conformal Array Antenna With High Gain for 5G Applications	H. Xu, B.-z. Zhang, J.-p. Duan, J. Cui, Y. Xu, Y. Tian, L. Yan, M. Xiong, and Q. Jia	2304
Improved Prediction of the Wideband Beam Pattern Shape of Antenna Array Based on Infinitesimal Dipole Modeling	Y.-D. Kim, S.-J. Yang, N.-H. Myung, and J.-W. Yu	2309
Combined Constrained Adaptive Sum and Difference Beamforming in Monopulse Angle Estimation	L. Zhu, S. Qiu, and Y. Han	2314
Planar Pattern Switchable Antenna Using Phase Reconfigurable Synthesized Transmission Lines	H. N. Chu, G.-Y. Li, and T.-G. Ma	2319
Reconfigurable Phased Array Antenna Consisting of High-Gain High-Tilt Circularly Polarized Four-Arm Curl Elements for Near Horizon Scanning Satellite Applications	H. Zhou, A. Pal, A. Mehta, H. Nakano, A. Modigliana, T. Arampatzis, and P. Howland	2324
Millimeter-Wave Substrate-Based Dielectric Reflectarray	Y.-X. Sun and K. W. Leung	2329
In Vivo Testing of a Miniature 2.4/4.8 GHz Implantable Antenna in Postmortem Human Subject	J. Blauert, Y.-S. Kang, and A. Kiourti	2334
On-Demand Band-Rejected Wideband Antenna Based on Peelable Resonator Membrane	R. Wang, M. Li, S. Raju, R. C. Roberts, M. Chan, and L. Jiang	2339
Dual Linearly Polarized Microstrip Antenna Using a Slot-Loaded TM ₅₀ Mode	Y. He, Y. Li, W. Sun, Z. Zhang, and P.-Y. Chen	2344
Dimensionality Reduction of the Polynomial Chaos Technique Based on the Method of Moments	C. Salis and T. Zygididis	2349
Impaired Array Diagnosis and Mitigation With Khatri–Rao Processing	D. Jiang, W.-Q. Wang, Z. Zheng, and S. Zhang	2354
Cramér–Rao Lower Bound on AoA Estimation Using an RF Lens-Embedded Antenna Array	J.-N. Shim, H. Park, C.-B. Chae, D. K. Kim, and Y. C. Eldar	2359
A Propagation Model for Mixed Paths Using Dyadic Green’s Functions: A Case Study Over the River for a City–River–Forest Path	D. K. N. da Silva, L. E. C. Eras, A. A. Moreira, L. M. Correia, F. J. B. Barros, and G. P. dos Santos Cavalcante	2364
A Study on Harmonic Power Calculation for Nonuniform Period Linear Time Modulated Arrays	I. Kanbaz, U. Yesilyurt, and E. Aksoy	2369
High-Gain Patch Antenna Based on Cylindrically Projected EBG Planes	D. Chen, W. Yang, and W. Che	2374
Perforated Lightweight Broadband Metamaterial Absorber Based on 3-D Printed Honeycomb	S. Ghosh and S. Lim	2379
Design of Bandwidth-Enhanced Platform-Mounted Electrically Small VHF Antennas Using the Characteristic-Mode Theory	R. Ma, T.-Y. Shih, R. Lian, and N. Behdad	2384
A Reduced Size Planar Grid Array Antenna for Automotive Radar Sensors	E. Arneri, F. Greco, L. Boccia, and G. Amendola	2389

Simulation Analysis of Electromagnetic Surface Wave Suppression by Soft Surfaces, Including Effects of Resistive and Active Elements.....	<i>C. Wang, D. Bisharat, S. Kim, E. Li, and D. F. Sievenpiper</i>	2394
Conformal Automotive Roof-Top Antenna Cavity With Increased Coverage to Vulnerable Road Users.....	<i>G. Artner, W. Kotterman, G. Del Galdo, and M. A. Hein</i>	2399
Design of Sharp Roll-Off Band Notch With Fragment-Type Pattern Etched on UWB Antenna.....	<i>Y. Du, X. Wu, J. Sidén, and G. Wang</i>	2404
Miniaturized High-Order-Mode Dipole Antennas Based on Spoof Surface Plasmon Polaritons.....	<i>Y. Yang, Z. Li, S. Wang, X. Chen, J. Wang, and Y. J. Guo</i>	2409
A Wideband, Low-Profile Log-Periodic Monopole Array With End-Fire Scanning Beams.....	<i>G. Liu, H. Li, Y. Chen, H. He, S. Gao, and S. Yang</i>	2414
Including the Effects of Curvature in the Cavity Model and New Manufacturing Considerations for Cylindrical Microstrip Antennas.....	<i>D. F. M. Boada and D. C. do Nascimento</i>	2419
Feeding Coils Design for TE-Polarized Bessel Antenna to Generate Rotationally Symmetric Magnetic Field Distribution.....	<i>P. Lu, A. Bréard, J. Huillery, X.-S. Yang, and D. Voyer</i>	2424
A W-Shaped Antenna With Spatial Polarization Variation for Direction Finding.....	<i>S. Choi and K. Sarabandi</i>	2429
Beamforming Optimization for Time-Modulated Circular-Aperture Grid Array With DE Algorithm.....	<i>Z. J. Jiang, S. Zhao, Y. Chen, and T. J. Cui</i>	2434
Subarray Decomposition for Radiation Measurement of High-Power Excited Electrically Large Phased Arrays of Antennas in Regular Anechoic Chambers.....	<i>H.-T. Chou, H.-J. Huang, D.-Y. Cheng, S.-C. Tuan, and H.-Y. Chen</i>	2439
A Compact Hybrid-Fed Microstrip Antenna for Harmonics-Based Radar and Sensor Systems.....	<i>L. Zhu, N. Alkhalidi, H. M. Kadry, S. Liao, and P.-Y. Chen</i>	2444
Propagation Loss Reduction Between On-Body Antennas by Using a Conductive Strip Line.....	<i>T. T. Lan and H. Arai</i>	2449
A Broadband Circularly Polarized Wide-Slot Antenna With a Miniaturized Footprint.....	<i>U. Ullah and S. Koziel</i>	2454
Compact Ring Slot Antenna With Harmonic Suppression.....	<i>W. Li, Y. Wang, B. You, Z. Shi, and Q. H. Liu</i>	2459
A Tilted-D-Shaped Monopole Antenna With Wide Dual-Band Dual-Sense Circular Polarization....	<i>A. Altaf and M. Seo</i>	2464
Dual-Band Filtering Antenna With Novel Transmission Zero Characteristics.....	<i>K. Dhawaj, L. J. Jiang, and T. Itoh</i>	2469
A Capacitive Loading Method for Turning a Single-Band Antenna Into Dual-Band for Wireless Terminal Applications.....	<i>J. Sui and K.-L. Wu</i>	2474
Tapered Unit Cell Control of a Sinusoidally Modulated Reactance Surface Antenna.....	<i>D. Yang and S. Nam</i>	2479
In-Body and Off-Body Channel Modeling for Future Leadless Cardiac Pacemakers Based on Phantom and Animal Experiments.....	<i>P. Bose, A. Khaleghi, and I. Balasingham</i>	2484
Polarization-Insensitive Broadband Multilayered Absorber Using Screen Printed Patterns of Resistive Ink.....	<i>Y. Tayde, M. Saikia, K. V. Srivastava, and S. A. Ramakrishna</i>	2489
Switchable Complementary Diamond-Ring-Shaped Metasurface for Radome Application.....	<i>H. Xu, K. Bi, Y. Hao, J. Zhang, J. Xu, J. Dai, K. Xu, and J. Zhou</i>	2494
Closely Spaced Broadband MIMO Differential Filtering Slotline Antenna With CM Suppression.....	<i>H.-W. Deng, T. Xu, Y.-F. Xue, F. Liu, and L. Sun</i>	2498
Surface Wave Based Underwater Radio Communication.....	<i>I. I. Smolyaninov, Q. Balzano, C. C. Davis, and D. Young</i>	2503
Time-Modulated Multibeam Phased Arrays With Periodic Nyquist Pulses.....	<i>R. Maneiro-Catoira, J. Brégains, J. A. García-Naya, and L. Castedo</i>	2508
Multiple Beam Parasitic Array Radiator Antenna for 2.4 GHz WLAN Applications.....	<i>Q. Liang, B. Sun, and G. Zhou</i>	2513
A Wideband FSS Based on Vias for Communication Systems.....	<i>Y. Ma, W. Wu, Y. Yuan, X. Zhang, and N. Yuan</i>	2517

COMMENTS AND REPLIES

Comments on “Optimization of Sparse Frequency Diverse Array With Time-Invariant Spatial-Focusing Beampattern”..	<i>M. Fartookzadeh</i>	2521
Reply to “Comments on ‘Optimization of Sparse Frequency Diverse Array With Time-Invariant Spatial-Focusing Beampattern’”.....	<i>Y.-Q. Yang, H. Wang, H.-Q. Wang, S.-Q. Gu, D.-L. Xu, and S.-L. Quan</i>	2522

2018 List of Reviewers.....		2523
-----------------------------	--	------

IEEE ANTENNAS AND WIRELESS PROPAGATION LETTERS

All members of the IEEE are eligible for membership in the Antennas and Propagation Society and will have access to this LETTERS upon payment of the annual Society membership fee of \$15.00. For information on joining, write to the IEEE at the address below. *Member copies of Transactions/Journals are for personal use only.*

CHRISTOPHE FUMEAUX, *Editor-in-Chief*
School of Electrical & Electronic Engineering
The University of Adelaide, Adelaide, SA 5005, Australia
e-mail: awpl@ieeeps.org
<http://awpl.eleceng.adelaide.edu.au/>

CLAIRE SIDERI, *Editorial Assistant*
e-mail: awpl@ieeeps.org

Senior Associate Editors

AMIN ABBOSH
University of Queensland, Australia

TZYH-GHUANG MA
National Taiwan University of Science and Technology

Associate Editors

BO AI
Beijing Jiaotong University
AKRAM ALOMAINY
Queen Mary University of London
GIANDOMENICO AMENDOLA
Universita' della Calabria
MAX AMMANN
Dublin Institute of Technology
FRANCESCO ANDRIULLI
Institute Mines-Telecom/Telecom Bretagne
MARCO ANTONIADES
University of Cyprus
BENJAMIN BRAATEN
North Dakota State University
TIM BROWN
University of Surrey
SHIH-YUAN CHEN
National Taiwan University
XIAOMING CHEN
Xi'an Jiaotong University

YU JIAN CHENG
University of Electronic Science and
Technology of China
COSTAS C. CONSTANTINOU
University of Birmingham
SANDRA COSTANZO
University of Calabria
JOSEPH COSTANTINE
American University of Beirut
MARÍA ELENA DE COS GÓMEZ
University of Oviedo
FRANCISCO FALCONE
University of Massachusetts Amherst
GEORGE GOUSSETIS
Heriot-Watt University
DEBATOSH GUHA
University of Calcutta
YONGXIN GUO
National University of Singapore
GEORGE HANSON
University of Wisconsin-Milwaukee

YI HUANG
University of Liverpool
DO-HOON KWON
University of Massachusetts Amherst
YUE LI
Tsinghua University
LOIC MARKLEY
University of British Columbia,
Okanagan
LADISLAV MATEKOVITS
Politecnico di Torino
PAOLO NEPA
Universit of Pisa
SIMA NOGHANIAN
University of North Dakota
GIACOMO OLIVERI
University of Trento
PEIYUAN QIN
University of Technology Sydney
ANIL KUMAR RAMRAKHYANI
Google Life Sciences

SUDHAKAR RAO
Northrop Grumman Aerospace Systems
SATISH KUMAR SHARMA
San Diego State University
CHOW-YEN-DESMOND SIM
Feng Chia University
JIMING SONG
Iowa State University
DIANE TITZ
University of Nice
JAYANTI VENKATARAMAN
Rochester Institute of Technology
HANYANG WANG
Huawei Technologies
JAMES WEST
Oklahoma State University
HANG WONG
City University of Hong Kong
HAO XIN
University of Arizona
ALEXANDER YAKOVLEV
University of Mississippi

IEEE Officers

JAMES A. JEFFERIES, *President*
JOSÉ M. F. MOURA, *President-Elect*
WILLIAM P. WALSH, *Secretary*
JOSEPH V. LILLIE, *Treasurer*
KAREN BARTLESON, *Past President*

WITOLD M. KINSNER, *Vice President, Educational Activities*
SAMIR M. EL-GHAZALY, *Vice President, Publication Services And Products*
MARTIN BASTIAANS, *Vice President, Member and Geographic Activities*
FORREST D. "DON" WRIGHT, *President, Standards Association*
SUSAN "KATHY" LAND, *Vice President, Technical Activities*
SANDRA "CANDY" ROBINSON, *President, IEEE-USA*

JOHN Y. HUNG, *Director, Division VI*

IEEE Executive Staff

STEPHEN P. WELBY, *Executive Director & Chief Operating Officer*
THOMAS SIEGERT, *Business Administration*
JULIE EVE COZIN, *Corporate Governance*
DONNA HOURICAN, *Corporate Strategy*
JAMIE MOESCH, *Educational Activities*
JACK BAILEY, *General Counsel & Chief Compliance Officer*
VACANT, *Human Resources*
CHRIS BRANTLEY, *IEEE-USA*

CHERIF AMIRAT, *Information Technology*
KAREN HAWKINS, *Marketing*
CECELIA JANKOWSKI, *Member and Geographic Activities*
MICHAEL FORSTER, *Publications*
KONSTANTINOS KARACHALIOS, *Standards Association*
MARY WARD-CALLAN, *Technical Activities*

IEEE Periodicals

Transactions/Journals Department

Senior Director, Publishing Operations: DAWN MELLEY
Director, Editorial Services: KEVIN LISANKIE *Director, Production Services:* PETER M. TUOHY
Associate Director, Editorial Services: JEFFREY E. CICHOCKI *Associate Director, Information Conversion and Editorial Support:* NEELAM KHINVASARA
Managing Editor: PATRICK J. KEMPF *Journals Coordinator:* CAMILLE VENTURA

IEEE ANTENNAS AND WIRELESS PROPAGATION LETTERS (ISSN 1536-1225) is published annually by The Institute of Electrical and Electronics Engineers, Inc. Responsibility for the contents rests upon the authors and not upon the IEEE, the Society/Council, or its members. **IEEE Corporate Office:** 3 Park Avenue, 17th Floor, New York, NY 10016-5997. **IEEE Operations Center:** 445 Hoes Lane, Piscataway, NJ 08854-4141. **NJ Telephone:** +1 732 981 0060. **Price/Publication Information:** Individual copies: IEEE members \$20.00 (first copy only), nonmembers \$70.00 per copy. (Note: Postage and handling charge not included.) Member and nonmember subscription prices available on request. **Copyright and Reprint Permissions:** Abstracting is permitted with credit to the source. Libraries are permitted to photocopy for private use of patrons, provided the per-copy fee of \$31.00 is paid through the Copyright Clearance Center, 222 Rosewood Drive, Danvers, MA 01923. For all other copying, reprint, or republication permission, write to Copyrights and Permissions Department, IEEE Publications Administration, 445 Hoes Lane, Piscataway, NJ 08854-4141. Copyright © 2018 by The Institute of Electrical and Electronics Engineers, Inc. All rights reserved. IEEE prohibits discrimination, harassment and bullying. For more information visit <http://www.ieee.org/nondiscrimination>. Printed in U.S.A.

Mutual Coupling Reduction for a UWB Coplanar Vivaldi Array by a Truncated and Corrugated Slot

Nurhayati [✉], *Student Member, IEEE*, Gamantyo Hendrantoro [✉], *Senior Member, IEEE*,
Takeshi Fukusako [✉], *Senior Member, IEEE*, and Eko Setijadi, *Member, IEEE*

Abstract—This letter reports mutual coupling reduction in an ultrawideband coplanar Vivaldi array (CVA) by incorporating truncated and corrugated slot at the border between adjacent elements. An examination of CVAs shows that mutual coupling in the E-plane is more significant than in the H-plane. Subsequently, arrays using exponential and rectangular corrugated slot are compared with those without a slot structure through the simulation of a surface current distribution. A novel exponential corrugated truncated (ECT) structure is implemented to improve a mutual coupling performance, while maintaining or even improving copolar field patterns. The results of simulation and measurement indicate that mutual coupling and return loss performance can be improved by controlling the length of corrugated structure and the distance of the slot structure from the center of the Vivaldi's tapered slot. The CVA achieves bandwidth ratio of 5:1, i.e., from 2 to 10 GHz. The ECT-CVA structure reduces mutual coupling to below -20 dB in a large portion of the whole band, shows 3.9–10.2 dBi gain over the entire band, increases a sidelobe level performance at 4–9 GHz compared to the CVA without slot structure.

Index Terms—Antenna array, corrugated antenna, mutual coupling, Vivaldi antenna.

I. INTRODUCTION

VIVALDI antenna was first proposed by Gibson [1] for large bandwidth and high directivity. Other advantages include ability in realizing a desired gain, beamwidth, and beam scanning, as well as practicability for an arrangement into an array. The minimum bandwidth requirement of 2:1 for an ultrawideband (UWB) antenna [2] can be fulfilled by Vivaldi, which has been used in such applications as void detection inside concrete, wearable communications, and sensing systems [3]–[7]. This letter focuses on the coplanar Vivaldi antenna that gives higher gain and more symmetrical radiation pattern than the antipodal Vivaldi antenna (AVA) [8].

Manuscript received August 11, 2018; revised September 19, 2018; accepted September 20, 2018. Date of publication October 1, 2018; date of current version November 29, 2018. This work was supported by the Indonesian Ministry of Research, Technology and Higher Education through the 2017 Peningkatan Kualitas Publikasi Internasional (PKPI) program. (*Corresponding author: Nurhayati.*)

Nurhayati is with the Department of Electrical Engineering, Institut Teknologi Sepuluh Nopember, Surabaya 60111, Indonesia, on leave from the Department of Electrical Engineering, Universitas Negeri Surabaya, Surabaya 60231, Indonesia (e-mail: nurhayati15@mhs.ee.its.ac.id; nurhayati@unesa.ac.id).

G. Hendrantoro and E. Setijadi are with the Department of Electrical Engineering, Institut Teknologi Sepuluh Nopember, Surabaya 60111, Indonesia (e-mail: gamantyo@ee.its.ac.id; ekoset@ee.its.ac.id).

T. Fukusako is with the Department of Computer Science and Communication Engineering, Kumamoto University, Kumamoto 860-8555, Japan (e-mail: fukusako@cs.kumamoto-u.ac.jp).

Digital Object Identifier 10.1109/LAWP.2018.2873115

Attempts have been made to realize Vivaldi with larger bandwidth and minimized dimension [9]–[11]. However, smaller antennas reduce efficiency and hardly yield return loss above 10 dB at lowest frequency. While in an array smaller elements can reduce grating lobe at high frequency, such elements can increase mutual coupling if the spacing is less than half wavelength of its lowest frequency, which in turn degrades radiation pattern and return loss.

Mutual coupling reduction techniques between non-Vivaldi elements have been reported, such as meander line [12], metamaterial [13], and strip wall [14], which are complex, employing either double layer or wall. Radiation pattern improvement by corrugated structure has been reported in [15] and [16], but mutual coupling induced has not been studied. Mutual coupling has been studied for the array of AVAs [17], but a return loss for each element and mutual coupling (given by S_{ij} , where $i \neq j$) have not been researched thoroughly.

A previous study [18] shows that the infinite array of the Vivaldi elements benefits from mutual coupling in terms of larger bandwidth. But some applications might only require finite array, for which mutual coupling and return loss at lower band are problematic. Accordingly, our main contribution is the study of mutual coupling and its reduction by applying various types of slot structure at the border between elements in coplanar Vivaldi arrays (CVAs) with limited number of elements built as continuous patch. The first part of this letter evaluates mutual coupling in such arrays, which demonstrates that mutual coupling in the E-plane is more significant than that in the H-plane, as presented in Section II.

The latter part of this letter discusses mutual coupling reduction in the E-plane for CVA by introducing slot structures at the border between adjacent elements oriented transverse to the direction of surface current, strengthened by corrugation and truncation. We compare arrays with different structures in terms of surface current distribution, return loss, mutual coupling, and copolar and cross-polar field patterns. We also provide equations for a length of the slot structure and its distance to the element's tapered slot that determines mutual coupling and return loss. Simulation using computer simulation technology (CST) and measurement show that arrays with exponential corrugated truncated (ECT) slot performs the best in mutual coupling, gain, and sidelobe level (SLL). This is discussed in Section III, while the overall conclusion is given in Section IV.

II. MUTUAL COUPLING IN CVA

The Vivaldi elements are designed as in Fig. 1 on FR4 materials with dielectric constant of 4.6, substrate thickness of 1.6 mm,

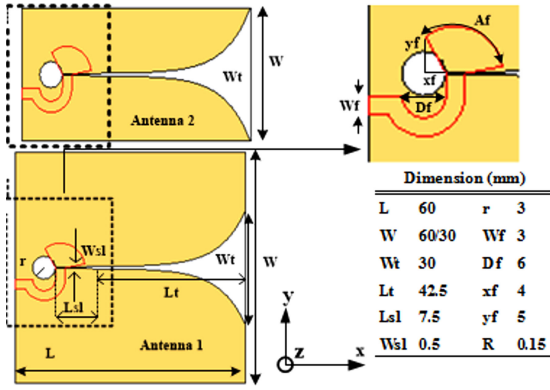
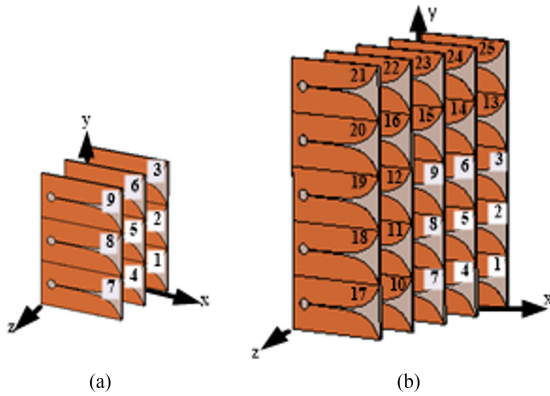


Fig. 1. Dimension of coplanar Vivaldi antenna elements.


 Fig. 2. CVA with dimensions (a) 3×3 and (b) 5×5 , which is an extension from 3×3 .

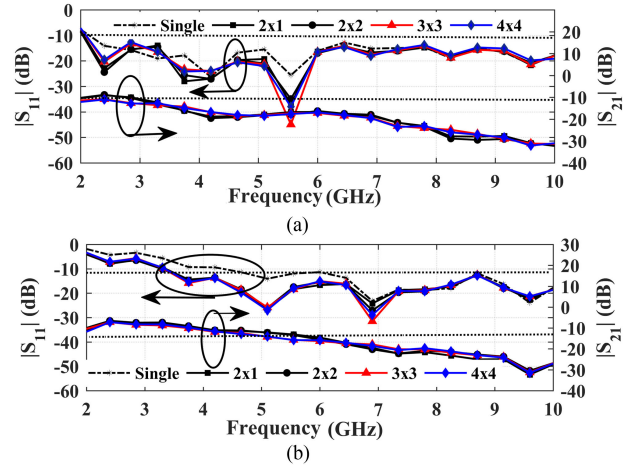
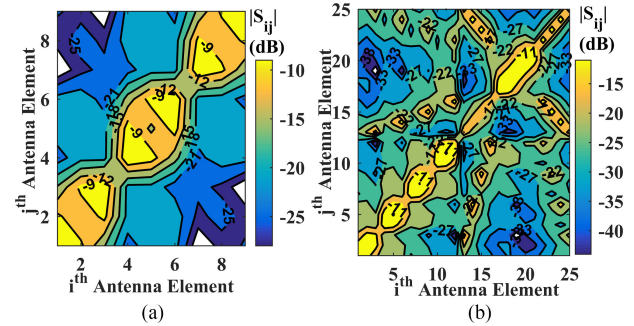
and copper thickness of 0.035 mm. The 60 mm \times 60 mm element has bandwidth ratio of 5:1, i.e., return loss is better than 10 dB in the 2–10 GHz range, typical of UWB antennas. The tapered slot of Vivaldi can be designed as [17]

$$y = C_1 e^{Rx} + C_2, \quad C_1 = \frac{y_2 - y_1}{e^{Rx_2} - e^{Rx_1}},$$

$$C_2 = \frac{y_1 e^{Rx_2} - y_2 e^{Rx_1}}{e^{Rx_2} - e^{Rx_1}} \quad (1)$$

where y denotes the tapered slot curve, x_1 , y_1 , x_2 , and y_2 the coordinates of the start and end of tapered slot's slope.

CVAs with different dimensions in Fig. 2 are analyzed to get scattering a parameter performance in Figs. 3 and 4 before discussing a mutual coupling method. The center-to-center spacing of 30 mm at 2 GHz for an array structure with continuous patch is equivalent to element width of $0.2 \lambda_0$, but 60 mm is equivalent to element width of $0.4 \lambda_0$. Both antennas have different element widths with other parameters fixed. It yields high mutual coupling ($S_{21} > -10$ dB) around the lower end frequency. Fig. 3(a) and (b) shows S_{11} and S_{21} performance in decibel scale at 2 GHz for element width of 60 mm (0.4λ) and 30 mm (0.2λ), respectively. With finite yet increasing number of elements, the array with 30 mm (0.2λ) element width shows increasing bandwidth as shown by the S_{11} curve in the upper side of Fig. 3(b), but the mutual coupling remains high. Smaller elements with narrower radiator patch and narrower mouth opening of tapered slot


 Fig. 3. S_{11} and S_{21} performance of arrays with (a) $0.4 \lambda \times 0.4 \lambda$ elements and (b) $0.2 \lambda \times 0.4 \lambda$ elements.

 Fig. 4. Contour plot of scattering parameter (S_{ij}) for j th element to i th element for (a) 3×3 array and (b) 5×5 array, respectively.

shifts upward the lower bound of operating frequency range at which S_{11} is below -10 dB. To obtain low return loss, a Vivaldi antenna is usually designed with slot width of one wavelength [19]. For smaller element width, if the number of elements in the array is gradually increasing to infinity, the bandwidth increases because of a coupling environment. However, in Fig. 2, those arrays are just simulated with the finite number of elements, and therefore, the lowest frequency is still high. In contrast, in Fig. 3(a), for arrays with 60 mm (0.4λ) element width, the bandwidth does not increase significantly with more elements. Smaller spacing between feeding points in the E-plane changes the coupling environment so that anomalies of impedance occur. However, the increasing number of element can increase the bandwidth.

The S -parameters at 2.4 GHz of 3×3 arrays in Fig. 4(a) and 5×5 arrays in Fig. 4(b) are shown in contour plots for element width of 0.2λ with the numbering of antenna element is the same as a port number of the antenna given in Fig. 2. They reveal that increasing number of elements enhances the performance of a return loss as well as a mutual coupling parameter. It can be seen for the 3×3 array, S_{33} is -9 dB, while the 5×5 array has S_{33} of -11 dB. For the 3×3 array, S_{98} is -9 dB but for the 5×5 array, S_{98} is -11 dB, where S_{ij} for $i \neq j$ is the coupling from j th element to i th element for an arrangement shown in Fig. 2. By increasing the number of elements, mutual scattering can be reduced because it is induced by coupling from elements on

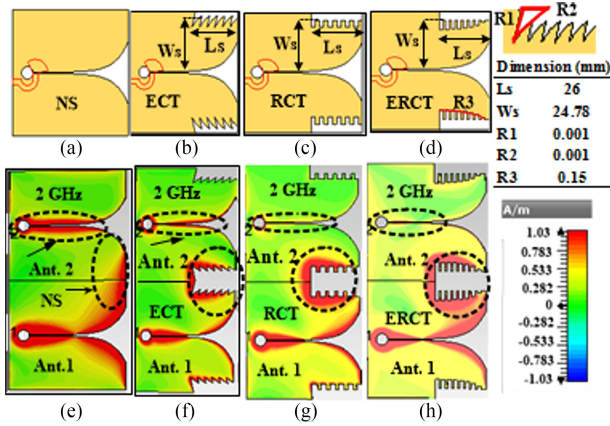


Fig. 5. Geometry of the Vivaldi element with slot structures. (a) NS, (b) ECT, (c) RCT, and (d) ERCT with their corresponding current distribution in (e)–(h).

all sides. In the E-plane, mutual coupling appears to be larger than it is in the H-plane. For the 5×5 array, in the E-plane, S_{56} is around -11 dB, which is higher than mutual coupling in the H-plane with S_{58} of around -22 dB. In the E-plane, surface current flows in the adjacent element, which causes coupling between elements, whereas in the H-plane, coupling is induced by electric field through the air. The diagonal of contour plot shows $S_{ij} = S_{ji}$. Over all, these observations indicate that mutual coupling is a bigger issue than return loss in CVAs, with greater impact shown in the E-plane than the H-plane.

III. MUTUAL COUPLING REDUCTION

A. Vivaldi Antenna and Surface Current Performance

We consider several slot structures, i.e., straight, exponential, corrugated and truncated, or their combinations. Truncated slot has been used in [18] but how it reduces mutual coupling is not explained. Corrugated slots have been used in [15] and [16] for different purposes to improve radiation pattern, as well as in our previous work [20]. Aside from no slot structure (NS), there are three types of slot structure evaluated herein for mutual coupling reduction, as shown in Fig. 5, namely, ECT slot, rectangular corrugated truncated slot (RCT), and exponential RCT slot (ERCT). All structures are simulated with the same amplitude excitation with ideal (lossless) power divider connected to SubMiniature version A (SMA) connectors.

B. Surface Current Performance

Fig. 5 shows geometry of coplanar Vivaldi element and surface current in two element array when the lower antenna (antenna 1) is excited and the upper (antenna 2) is terminated at 2 GHz. Surface currents in NS array in Fig. 5(e) couple to the upper antenna, which is observable from the direction of the surface current in the areas encircled. This happens because there is no transverse structure in between the elements that disturbs the flow of the leaking surface current. In contrast, surface current on array with ECT in Fig. 5(f), RCT in Fig. 5(g), ERCT in Fig. 5(h), concentrated along the slot structure at the border, thus, reducing the current that flows to the next element. To further enhance the current concentration around the slot structure and minimize the leakage, saw tooth corrugation can

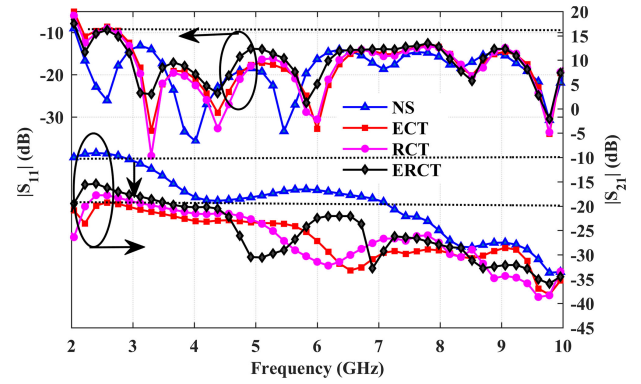


Fig. 6. S-parameters for arrays with various structures.

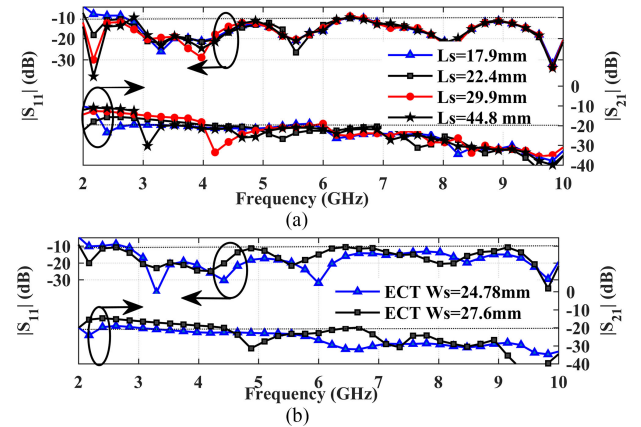


Fig. 7. S-parameters. (a) Varying L_s . (b) Varying W_s .

be applied to the slot, for which higher corrugated slope gives better result. In the corrugated slot, surface currents propagate to adjacent element along a longer path than in the straight structure and also crash each other, thereby increasing isolation.

C. Scattering Parameter Performance

Fig. 6 compares S_{11} and S_{21} of Vivaldi arrays with various slot structures. The array structures in the order of superiority in S_{11} performance at 2.2 GHz are ERCT, RCT, ECT, and NS. Better isolation is achieved with ECT, RCT, ERCT, and NS in the descending order of superiority at around 4 GHz. The best isolation is achieved for ECT. Accordingly, it suggests that corrugated structure should be used with truncation for the isolation.

Increasing L_s with a constant $W_s = 0.5 \lambda_g$ (at 4 GHz) can improve return loss performance but reduce isolation as shown in Fig. 7(a). Longer L_s makes surface current spread along truncated slot over longer path and subsequently make the U-turn. Some of the surface current directly flows towards the area in the beginning of tapered slot in the adjacent element and reduces isolation. In contrast, the shorter corrugated truncated slot makes some of surface current spread near opening of tapered slot in the excited element and escalates return loss at lower frequency. After the surface current makes a U-turn to the next element, it flows to the center slot with longer trajectory that enhances isolation. S_{11} performance below -10 dB can be reached from 2 to 10 GHz by setting the length of L_s

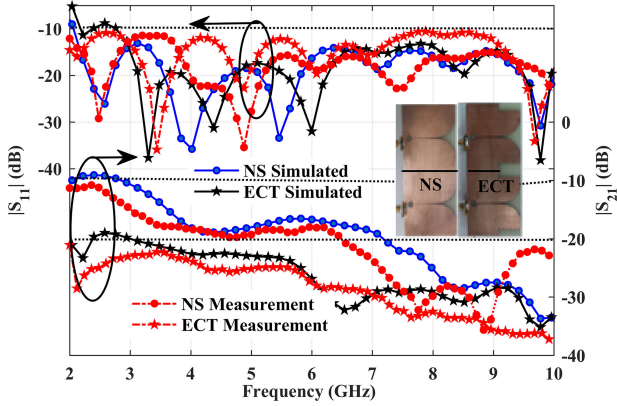


Fig. 8. Simulation and measurement S_{11} and S_{21} : NS and ECT.

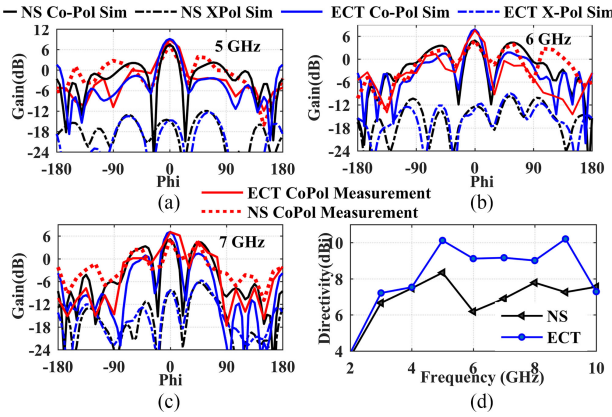


Fig. 9. Simulation and measurement results of copolar gain and simulation of cross-polar gain in the E-plane at (a) 5 GHz, (b) 6 GHz, and (c) 7 GHz. (d) Directivity at 2–10 GHz for ECT and NS.

to $0.5 \lambda_g$ with guided wavelength λ_g obtained from any value of f (GHz) where $f_L \leq f \leq (f_c - 2)$ and setting W_s to $0.5 \lambda_g$ where $f_L + 1 < f < (f_c - 2)$, with f_L and f_c is the lowest and the center frequency, respectively. This step gives the rule for minimum and maximum dimensions of L_s and W_s as shown in Fig. 5. By considering effective dielectric [16], the value of L_s and W_s should be set as

$$L_s \text{ or } W_s = 0.5\lambda_g = \frac{c}{2f(\sqrt{\epsilon_{eff}})} = \frac{\sqrt{2}\lambda}{2\sqrt{\epsilon_r + 1}}. \quad (2)$$

S_{11} and S_{21} for ECT with different values of W_s with a constant $L_s = 0.5 \lambda_g$ (at 3.5 GHz) are shown in Fig. 7(b). Smaller W_s appears to reduce a return loss performance but leads to higher isolation in both structures. To comply return loss requirement with smaller W_s , larger L_s can be used. Results of simulation and measurement of S_{11} and S_{21} for array with ECT and NS are presented in Fig. 8. By simulation, at 2.16 GHz, the arrays without slot yield S_{21} of -9.34 dB, whereas those with ECT give S_{21} of -24.19 dB. It is found that both simulation and measurement show consistency.

D. Radiation Pattern Performance

Fig. 9 compares simulation and measurement (see Fig. 10) results of a copolar gain and simulation of a cross-polar field

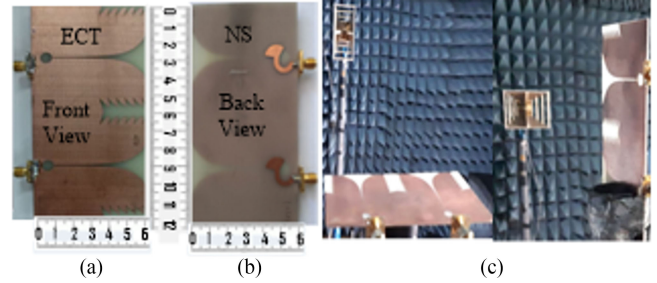


Fig. 10. Fabricated antenna. (a) ECT, (b) NS, and (c) ECT measurement.

TABLE I
COMPARISON OF ECT AND NS ARRAYS

f (GHz)	Dir (dBi)		Co-Pol (dB)		X-Pol (dB)		SLL(dB)		$ S_{21} $ (dB)	
	ECT	NS	ECT	NS	ECT	NS	ECT	NS	ECT	NS
2	3.9	3.7	3.5	3.3	-26	-22	-7.2	-7.2	-20	-9.8
3	7.2	6.7	6.8	6	-17	-15	-7.8	-8.7	-16	-11
4	7.5	7.5	6.8	6.7	-15	-14	-6.3	-5.3	-18	-18
5	10.1	8.3	9.1	7.4	-12	-12	-7.5	-5.3	-29	-18
6	9.1	6.2	7.8	4.8	-9	-9	-6	-1.6	-23	-17
7	9.2	6.9	7.1	5.1	-5.7	-6	-5.8	-2.1	-29	-19
8	9	7.8	6.6	5.8	-4	-4	-3.3	-2.8	-27	-25
9	10.2	7.3	7.1	4.9	-2.5	-3	-6.9	-1.2	-30	-28
10	7.3	6.6	0.7	-0.5	3.8	3	-1.6	-1	-34	-33

pattern in the E-plane between ECT-CVA and NS-CVA. The arrays generally preserve the wideband directivity as shown in Fig. 9(d). Radiation pattern and S_{21} performance of arrays with ECT and NS at various frequencies are shown in Table I. Directivity, copolar gain and S_{21} of ECT-CVA is better than NS over the whole band of 2–10 GHz, whereas the cross-polar gain for ECT is better than NS in the lower end frequency. ECT only improves SLL at 4–9 GHz, while at 10 GHz, array with element width of 60 mm has center-to-center spacing of $2 \lambda_0$, which yields grating lobes. A corrugated slot in antenna focuses electric field and enhances surface current over the whole patch, thus, improving directivity and radiation pattern. There are tradeoff between return loss, isolation, and SLL performance in an UWB antenna, which is influenced by the geometry of the antenna, feeding shape, patch design, and substrate.

IV. CONCLUSION

We have found that mutual coupling in UWB-CVA is more prevalent in E-plane than in H-plane. A family of mutual coupling reduction methods for CVA with various slot structures at the edges of adjacent elements has subsequently been demonstrated. Generally, the reduction of mutual coupling is achieved by placing a slot structure transverse to the direction of surface current at the border between elements to reduce surface current flowing to the next. The ECT structure is effective to improve isolation in all bands, especially at lower frequency, directivity in the whole band of 2–10 GHz, and SLL in 4–9 GHz. Therefore, it can be applied for the UWB CVA antenna application.

REFERENCES

- [1] P. J. Gibson, "The Vivaldi aerial," in *Proc. 9th Eur. Conf. Microw.*, Brighton, U. K., Sep. 1979, pp. 101–105.
- [2] R. L. Haupt, *Antenna Arrays: A Computational Approach*. New York, NY, USA: Wiley, 2010.
- [3] M. Moosazadeh, S. Kharkovsky, and J. T. Case, "Miniaturized UWB antipodal Vivaldi antenna and its application for detection of void inside concrete specimens," *IEEE Antennas Wireless Propag. Lett.*, vol. 16, pp. 1317–1320, 2017.
- [4] Q. H. Abbasi, M. U. Rehman, X. Yang, A. Alomainy, K. Qaraqe, and E. Serpedin, "Ultrawideband band-notched flexible antenna for wearable applications," *IEEE Antennas Wireless Propag. Lett.*, vol. 12, pp. 1606–1609, 2013.
- [5] R. Natarajan, J. V. George, M. Kanagasabai, and A. K. Shrivastav, "A compact antipodal Vivaldi antenna for UWB applications," *IEEE Antennas Wireless Propag. Lett.*, vol. 14, pp. 1557–1560, 2015.
- [6] S. Chamaani, M. S. Abrishamian, and S. A. Mirtaheri, "Time-domain design of UWB Vivaldi antenna array using multiobjective particle swarm optimization," *IEEE Antennas Wireless Propag. Lett.*, vol. 5, pp. 666–669, 2010.
- [7] J. Wu, Z. Zhao, Z. Nie, and Q.-H. Liu, "A printed UWB Vivaldi antenna using stepped connection structure between slotline and tapered patches," *IEEE Antennas Wireless Propag. Lett.*, vol. 13, pp. 698–701, 2014.
- [8] J. Puskely, J. Lacik, Z. Raida, and H. Arthaber, "High gain dielectric-loaded Vivaldi antenna for Ka-band application," *IEEE Antennas Wireless Propag. Lett.*, vol. 15, pp. 2004–2007, 2016.
- [9] D. Yang, S. Liu, and D. Geng, "A miniaturized ultra-wideband Vivaldi antenna with low cross polarization," *IEEE Access*, vol. 5, pp. 23352–23357, 2017.
- [10] G. Teni, N. Zhang, J. Qiu, and P. Zhang, "Research on a novel miniaturized antipodal Vivaldi antenna with improved radiation," *IEEE Antennas Wireless Propag. Lett.*, vol. 12, pp. 417–420, 2013.
- [11] A. Z. Hood, T. Karocolak, and E. Topsakal, "A small antipodal Vivaldi antenna for ultrawide-band applications," *IEEE Antennas Wireless Propag. Lett.*, vol. 7, pp. 656–660, 2008.
- [12] A. O. Boryszenko and D. H. Schaubert, "Physical aspects of mutual coupling in infinite broadband tapered slot (Vivaldi) arrays," in *Proc. 5th Int. Conf. Antenna Theory Tech.*, Kiev, Ukraine, May 2005, pp. 74–79.
- [13] S. Hwangbo, H. Y. Yang, and Y. K. Yoon, "Mutual coupling reduction using micromachined complementary meander-line slots for a patch array antenna," *IEEE Antennas Wireless Propag. Lett.*, vol. 16, pp. 1667–1670, 2017.
- [14] R. Hafezifard, M. N. Moghadasi, J. R. Mohassel, and R. A. Sadeghzadeh, "Mutual coupling reduction for two closely meander line antennas using metamaterial substrate," *IEEE Antennas Wireless Propag. Lett.*, vol. 15, pp. 40–43, 2016.
- [15] H. Qi, L. Liu, X. Yin, H. Zhao, and W. J. Kulesza, "Mutual coupling suppression between two closely spaced microstrip antennas with an asymmetrical coplanar strip wall," *IEEE Antennas Wireless Propag. Lett.*, vol. 15, pp. 191–194, 2016.
- [16] M. Abbak, M. N. Akinci, M. Cayoren, and I. Akduman, "Experimental microwave imaging with a novel corrugated Vivaldi antenna," *IEEE Trans. Antennas Propag.*, vol. 65, no. 6, pp. 3302–3307, Jun. 2017.
- [17] A. Oliveira, M. Perotoni, S. Kofuji, and J. Justo, "A palm tree antipodal Vivaldi antenna with exponential slot edge for improved radiation pattern," *IEEE Antennas Wireless Propag. Lett.*, vol. 14, pp. 1334–1337, 2015.
- [18] C. Zhang, M. Kuhri, M. Mahfouz, and E. Fathy, "Planar antipodal Vivaldi antenna array configuration for low cross-polarization and reduced mutual coupling performance," in *Proc. Int. Symp. IEEE Antennas Propag. Soc.*, 2007, pp. 725–728.
- [19] C. A. Balanis, *Modern Antenna Handbook*. New York, NY, USA: Wiley, 2008.
- [20] Nurhayati, G. Hendrantoro, and E. Setijadi, "Mutual coupling and radiation pattern of Vivaldi antenna with slit," in *Proc. 3rd Int. Conf. Commun. Inf. Process.*, Tokyo, Japan, Nov. 2017, pp. 296–300.

also developed by scimago:



SCIMAGO INSTITUTIONS RANKINGS

SJR

Scimago Journal & Country Rank

Enter Journal Title, ISSN or Publisher Name

[Home](#)[Journal Rankings](#)[Country Rankings](#)[Viz Tools](#)[Help](#)[About Us](#)

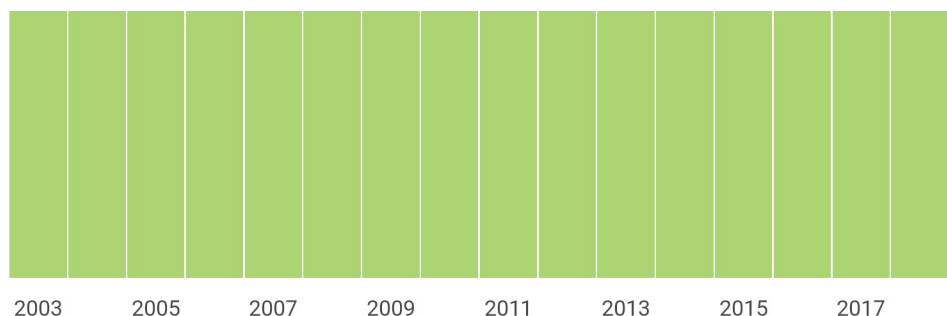
IEEE Antennas and Wireless Propagation Letters

Country	United States - SJR Ranking of United States	97
Subject Area and Category	Engineering Electrical and Electronic Engineering	
Publisher	Institute of Electrical and Electronics Engineers	H Index
Publication type	Journals	
ISSN	15361225	
Coverage	2002-ongoing	
Scope	A rapid-dissemination publication containing short manuscripts on new research results and technical developments in the areas of antennas and wireless propagation.	
	Homepage	
	Join the conversation about this journal	

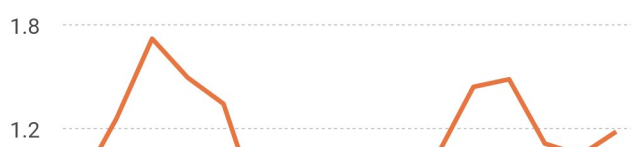
Quartiles



Electrical and Electronic Engineering



SJR

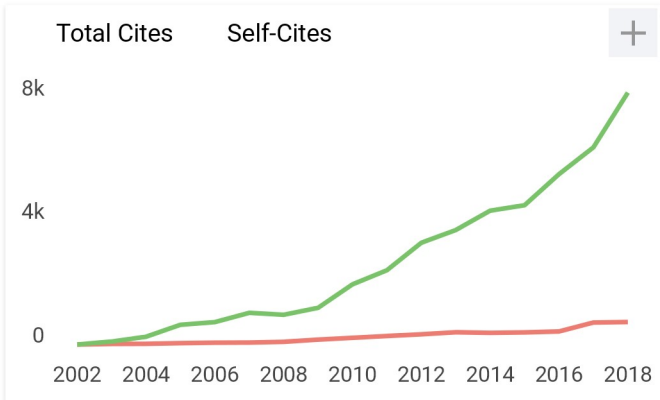


Citations per document

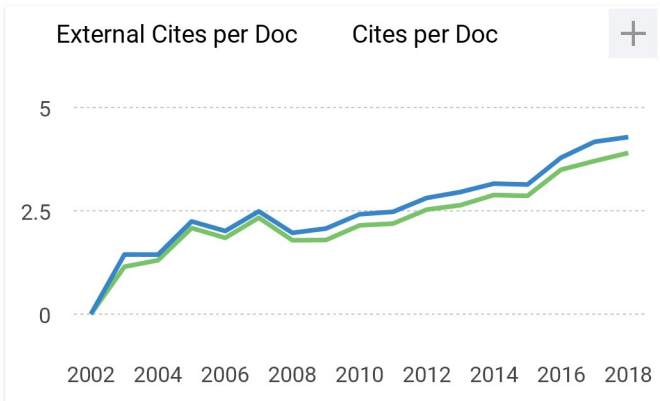


A

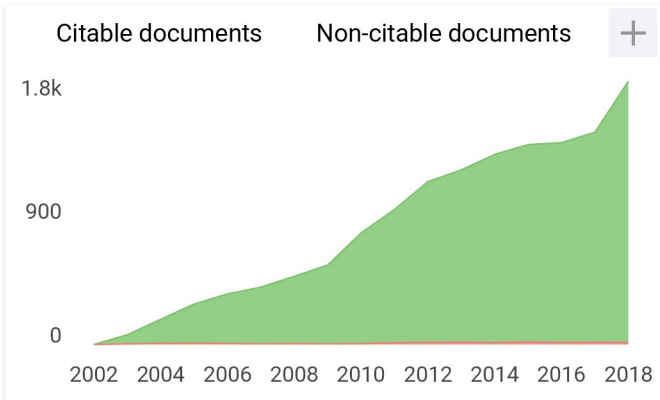
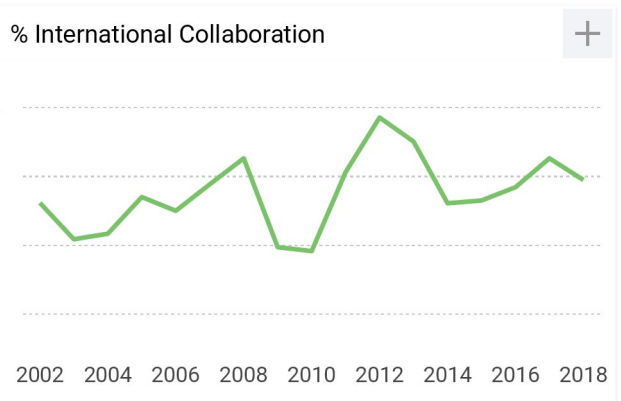
Dear administration,



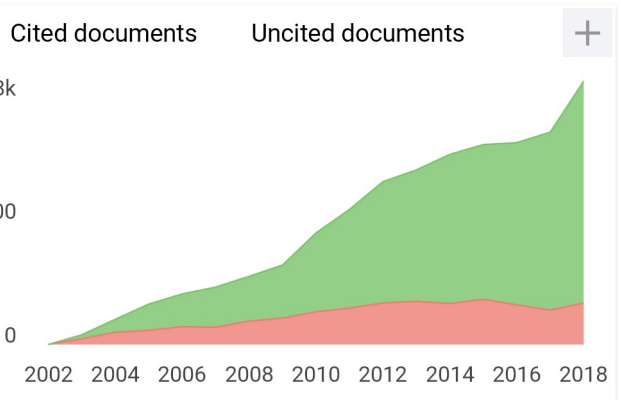
total below



total below



total below



IEEE Antennas and Wireless Propagation Letters

Q1 Electrical and Electronic Engineering
best quartile

SJR 2018
1.18

powered by scimagojr.com

← Show this widget in your own website

Just copy the code below and paste within your html code:

```
<a href="https://www.scimagojr.com/journalsearch.php?q=18894&tip=sid&clean=0" style="display: inline-block; border: 1px solid #ccc; padding: 2px 5px;">
    https://www.scimagojr.com/journalsearch.php?q=18894&tip=sid&clean=0
  </a>
```

document. SJR has been updated on June 1, 2018. Each year database and, according to that new information, indicators relating can change journal's quartile.

We're sorry for the inconvenience.

Leave a comment

Name

Email

(will not be published)

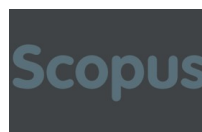
 Saya bukan robot
reCAPTCHA
Privasi - Persyaratan**Submit**

The users of Scimago Journal & Country Rank have the possibility to dialogue through comments linked to a specific journal. The purpose is to have a forum in which general doubts about the processes of publication in the journal, experiences and other issues derived from the publication of papers are resolved. For topics on particular articles, maintain the dialogue through the usual channels with your editor.

Developed by:



Powered by:



Follow us on @ScimagoJR

Scimago Lab, Copyright 2007-2019. Data Source: Scopus®

EST MODUS IN REBUS
Horatio (Satire 1.1.106)

